

## AN ATTEMPT TO DETECT FAINT OBJECTS NEAR QUASI-STELLAR OBJECTS WITH LOW-REDSHIFT ABSORPTION SYSTEMS

RAY J. WEYMANN,\* TODD A. BOROSON,\* AND BRADLEY M. PETERSON\*  
 Steward Observatory, University of Arizona

AND

HARVEY R. BUTCHER

Kitt Peak National Observatory

Received 1978 May 2; accepted 1978 June 8

### ABSTRACT

The fields of six QSOs with low absorption-line redshifts ( $z_a \lesssim 0.6$ ) have been examined on deep photographs for possible intervening galaxy images. No images less than  $\sim 60$  kpc distant from the line of sight to the QSO (on the intervening hypothesis) were found. It is shown that unless the correlation between absorbing clouds and galaxies is substantially stronger than the galaxy-galaxy correlation, “field” galaxies will always be more numerous than “correlated” galaxies for cases of interest. We also conclude that for Stockton’s sample of low *emission* redshift QSOs, the QSO-galaxy correlation is stronger than the galaxy-galaxy correlation.

*Subject headings:* BL Lacertae objects — cosmology — quasars

### I. INTRODUCTION

The basic unanswered question in the study of QSO absorption lines is the physical location and origin of the absorbing material. If the QSOs are at the cosmological distances implied by their emission redshifts (see Stockton 1978), then at least some of the absorption lines must arise in intervening objects unassociated with the QSOs. At this time only one such case is conclusively established: the 21 cm and Ca II H and K absorption lines in 3C 232 which arise in the spiral galaxy NGC 3067 (Haschick and Burke 1975; Grewing and Mebold 1975; Boksenberg and Sargent 1978). In addition, it has been suggested that absorption may also be due to material ejected from the QSOs. The arguments for this hypothesis are statistical in nature; the large number and multiplicity of absorption systems seem to be inconsistent with any known type of intervening object (G. Burbidge *et al.* 1977). Moreover, QSOs such as PHL 5200 and RS 23 show P Cygni-type lines (Lynds 1967) which most likely indicate mass ejection from the QSOs. Indeed, it seems certain that both types of absorption exist.

The definitive test of the extrinsic nature of a particular absorption system is the direct detection of a galaxy near the line of sight and with the correct redshift. One approach to this test is to look for absorption in QSOs behind known galaxies or clusters of galaxies (Peterson 1978). The drawback to this method is that most known galaxies have redshifts less than  $\sim 0.2$ ; this limits ground-based observations to searches for Ca II H and K and H I 21 cm absorp-

tion. These lines are expected to be more difficult to detect than lines which become accessible at larger redshift, e.g., Mg II  $\lambda\lambda 2795, 2802$ . A second approach is essentially the inverse process—that is, to search for galaxies near QSOs with known absorption redshifts. In this paper, we report on a search for candidate objects near QSOs with low-redshift absorption systems.

The QSOs selected for the program were several objects known to have absorption-line redshifts  $z_a < 0.6$ . Above that value, detection and measurement of the galaxy redshifts become very difficult. However, PHL 938, with an absorption-line redshift of 0.613, was also included in the program, since there were no known absorption systems less than this when the project was begun.

In order to maximize galaxy signal-to-sky noise we used a red passband, as defined in the next section. We have calculated the expected magnitude and angular size of a typical absorbing galaxy at redshifts out to 0.6. From the Schechter (1976) luminosity function and Holmberg’s (1975) radius-luminosity relation, we find that the mean cross-section weighted luminosity of absorbing galaxies is  $7L^*/12$ , where  $L^*$  is the luminosity of a galaxy of absolute magnitude  $M_B(0) = -20.6$ . The results of this calculation are presented in Table 1.

We estimated *K*-corrections for our passband from the work of Pence (1976) and recent work of Coleman and Weedman (1978). No luminosity evolution corrections were applied, though we note that such corrections may be substantial at the largest redshifts considered (Tinsley 1976). For comparison, we estimate the brightness of the night sky to be 20.6 mag arcsec<sup>-2</sup> in our passband; this number is obtained by integrating the spectral energy distribution measured

\* Visiting Astronomer at Kitt Peak National Observatory, which is operated by AURA, Inc., under contract with the National Science Foundation.

TABLE 1  
EXPECTED MAGNITUDES AND DIAMETERS OF MEAN  
ABSORBING GALAXIES

$z$	$m_R$		$\theta$ (30 kpc)
	Elliptical	Spiral	
0.1.....	17.9	17.8	12"2
0.2.....	19.7	19.5	7"1
0.3.....	21.0	20.4	5"5
0.4.....	22.0	21.3	4"7
0.5.....	22.8	22.1	4"2
0.6.....	23.6	22.8	3"9

NOTE.—Magnitudes in passband  $R' = 6500\text{--}8500 \text{ \AA}$  of galaxies of luminosity  $7L^*/12$ ;  $M_B = -20$ ,  $M_{R'} = -21.5$ ;  $H_0 = 50 \text{ km s}^{-1} \text{ Mpc}^{-1}$ ,  $q_0 = \frac{1}{2}$ .

by Turnrose (1974) at Palomar. The magnitudes shown in Table 1 indicate that the signal-to-noise ratio required to detect galaxies at redshifts  $\lesssim 0.6$  can be attained by stacking several image-tube exposures. The recent development of the Interactive Picture Processing System (IPPS) greatly facilitates this technique.

In § II, we describe observations of five QSOs and one BL Lacertae object with well-established low-redshift absorption systems. In three cases we detected objects which warrant further study; we also describe additional data obtained on these objects in § II. In § III, we summarize our results and discuss their implications for the origin of the absorption lines.

## II. OBSERVATIONS

We obtained from one to 13 direct photographs of the program objects with the Steward Observatory 140 mm ITT image tube at the Cassegrain focus of the 2.3 m telescope. A summary of the observations is presented in Table 2. The passband was defined by an RG2 filter and the red cutoff of the extended S-20 photocathode ( $\sim 8500 \text{ \AA}$ ), except for PHL 938, in which an additional filter provided a red cutoff at  $\sim 7300 \text{ \AA}$ . The plate scale is  $10'' \text{ mm}^{-1}$  and the seeing was at all times better than  $1''.5$ . Between consecutive exposures of each object, the telescope was moved a few arcsec so that the fiber optics pattern would be displaced slightly and would tend to cancel when

many exposures were added. During the course of the program, three different emulsions were used; these are also listed in Table 2. The IIa-D plates were baked for 3 hours and the 127-04 plates were baked for 4 hours in  $N_2$  at  $65^\circ\text{C}$ .

We scanned the plates with the PDS microphotometer at KPNO, using a  $40 \mu\text{m}$  square aperture and  $40 \mu\text{m}$  steps. The area scanned on each plate was a square centered on the QSO and 512 pixels ( $\sim 200''$ ) on a side. We added the digitized pictures of each object with the IPPS (Wells 1975); we then displayed each composite picture and transferred it to 35 mm film. In each case, we set the gray scale of the display to maximize contrast at the sky level, thus enhancing the visibility of faint objects, but degrading the resolution of the original material. These pictures are presented as Figures 1–6. In each picture the QSO is identified; the numbered objects are discussed below.

We have estimated a limiting magnitude for each composite picture by converting the single pixel ( $0''.4$  square) standard deviation in the sky signal to an intensity relative to the assumed mean sky brightness ( $20.6 \text{ mag arcsec}^{-2}$  in our passband). This limiting magnitude represents roughly a  $5\sigma$  signal from an object of uniform brightness over a  $1''.2$  square. The resulting limiting magnitudes are presented in Table 2. Note that the limiting magnitudes are not merely a function of the number of plates stacked, but also depend upon the emulsion used and the density to which the individual plates were exposed. Needless to say, our estimates of the limiting magnitudes are quite uncertain.

Below we comment on the individual objects.

### a) 0058+019 = PHL 938

The search for direct evidence of an intervening galaxy producing the absorption system in this QSO is particularly relevant because of the coincidence of the Mg II  $\lambda\lambda 2795, 2802$  doublet in absorption and the C IV  $\lambda 1550$  emission line. This superposition has been interpreted as an example of line locking (Burbidge and Burbidge 1975), thus supportive of the intrinsic hypothesis for the origin of the absorption lines.

Object 1 in Figure 1 (Plate 6) is  $6''.7$  from the QSO. This corresponds to 51 kpc at the absorption redshift

TABLE 2  
QSOs OBSERVED

QSO	$z_{em}$	$z_a$	NO. PLATES/ EMULSION	LIMITING MAG	NEAREST OBJECT	
					arcsec	kpc at $z_a$
0058+019 (PHL 938).....	1.955	0.6128	13/IIa-D	24.8	6.7	51
0735+178.....	....	0.4240	1/127-04	21.8	10.6	144
0952+179.....	1.472	0.238	5/103a-D	22.5	14	67
			2/127-04			
1038+068.....	1.270	0.4414	2/103a-D	21.6	12.4	84
1229-021.....	1.042	0.3953	6/103a-D	22.5	19.6	125
			1/127-04			
1548+114b.....	1.901	0.429	6/103a-D	22.5	4.8	32
			1/127-04			

$z_a = 0.612$  (Burbidge, Lynds, and Stockton 1968; Peterson *et al.* 1977). A 4 m prime focus plate of PHL 938 in a blue passband (IIIa-J + GG385) was kindly lent to us by Dr. C. R. Lynds. This plate was also digitized and displayed on the IPPS. It is reproduced in Figure 2 (Plate 7). Object 1 is faintly visible on the blue plate; it is clearly quite red. Using simulated aperture photometry on the IPPS, we measured magnitudes for this object on the two plates. The zero point of our calibration is based on the intensities assumed for the sky in each band. These intensities were taken from Turnrose (1974) to be 21.6 mag arcsec<sup>-2</sup> in the blue band and 20.6 mag arcsec<sup>-2</sup> in the red band. Because of uncertainties in these values, our magnitudes are poorly determined, perhaps by as much as 1 mag. The color, however, depends only on the relative intensities of sky in the two bands, and thus is probably accurate to 0.5 mag. The magnitudes of object 1 we derive by this method are 22.9 mag in the blue band and 20.7 mag in the red band. We note that these magnitudes and their difference are consistent with those of an elliptical galaxy with luminosity  $L^*$  at a redshift of 0.6.

We have made two unsuccessful attempts to obtain spectra of object 1. In 1977 January, we obtained seven photographic image-tube spectrograms of object 1 with the 2.3 m telescope and the Boller and Chivens image-tube spectrograph by offsetting from PHL 938. The spectrograms were recorded at a reciprocal dispersion of 242 Å mm<sup>-1</sup> and cover the spectral range 4410–6650 Å; [O II] λ3727 and the Ca II H and K break fall in this region at a redshift of 0.61. The seven sky-subtracted spectra were added together. No obvious features are present. On 1977 August 9, one of us (T. A. B.) observed object 1 by using the SIT digital spectrograph at the Cassegrain focus of the Hale 5 m telescope. This observation covered the spectral region 3700–6800 Å at a resolution ~12 Å. The integration time was 4000 s. Again, no features were seen and in neither case was any positive signal above sky definitely detected.

b) *PKS 0735+178*

PKS 0735+178 is a highly variable BL Lacertae object with an absorption redshift of  $z_a = 0.424$  (Burbidge and Strittmatter 1972; Carswell *et al.* 1974; Peterson *et al.* 1977). We obtained only one plate of this object (Fig. 3 [Pl. 8]). Aside from a possible faint extension to the northwest (object 2), the nearest object appears stellar (object 3) and is 10".6 away from the QSO. The very bright appearance of 0735+178 at the time the plates were taken (~15 mag) makes detection of nearby faint objects very difficult.

c) *AO 0952+179*

The Arecibo occultation source 0952+179 is a small double radio source with a component separation of ~2".5 and component sizes of ~0".5 (Hazard, Gulkis, and Bray 1967). The radio source was identified by Kinman and Burbidge (1967) with a QSO which they found to have a redshift of  $z_{em} = 1.472$ .

However, the optical position of the QSO as given by Kinman and Burbidge is 8".4 east of the radio position. This discrepancy is 30 times the uncertainty in the radio position given by Hazard *et al.* We have remeasured the optical position of the QSO from a glass copy of the Palomar Sky Survey on the two-coordinate Grant measuring engine at KPNO, and we find that it is 14".7 ± 0".5 east of the radio position. Thus it seems unlikely that the radio centroid and optical QSO position apply to the same object.

As part of an ongoing survey of low- and intermediate-redshift QSOs (Weymann, Williams, and Peterson 1979), 0952+179 was observed with the Boller and Chivens spectrograph at the Steward 2.3 m telescope. Two spectrograms with 47 Å mm<sup>-1</sup> reciprocal dispersion were obtained, and both show a pair of lines at λ3460.4 ± 0.2 and λ3469.0 ± 0.8. This pair of lines has the correct separation to be the Mg II λλ2795, 2802 doublet at a redshift of 0.238. This is the smallest absorption redshift that has been found in a QSO, aside from the absorption system in 3C 232.

Our composite picture of this source is presented in Figure 4 (Plate 9). Object 4 is ~16" from the QSO (~76 kpc at  $z_a = 0.239$ ) at a position angle of ~330°. The reality of this feature appears likely because it appears on two independent stacks of plates, and appears only on plates of this object. Object 5 is ~14" from the QSO (~67 kpc at the absorption redshift) at position angle ~45°. Inspection of the Sky Survey plates indicated that this object is very blue. Dr. H. Spinrad kindly obtained a spectrum of this object with the Lick image-dissector scanner. A featureless continuum was observed over the range 4000–6800 Å. Monochromatic magnitudes measured from this spectrum are 20.2 mag at λ4500 and 19.6 mag at λ5500.

d) *1038+064 = 4C 06.41*

This QSO has an emission redshift of 1.270 and an absorption redshift  $z_a = 0.4414$  (E. Burbidge *et al.* 1977). In Figure 5 (Plate 10) we present the composite picture of the field of 4C 06.41. The nearest object to the QSO (object 6) lies 12".4 from the QSO, which corresponds to a projected distance of 84 kpc at the absorption redshift.

e) *PKS 1229-02*

PKS 1229-02 (Fig. 6 [Pl. 11]) has an emission redshift  $z_{em} = 1.042$  (Penston 1976) and an absorption redshift  $z_a = 0.3953$  (Peterson and Strittmatter 1978). The nearest object (7) is 19".6 away at position angle 140°. The angular separation corresponds to 125 kpc at the absorption redshift.

f) *1548+114 = 4C 11.50*

Figure 7 (Plate 12) shows the double QSO 1548+114. The brighter QSO, labeled *a*, has an emission redshift of 0.436; the fainter QSO, labeled *b*, has an emission redshift of 1.901 (Wampler *et al.*

1973) and a probable absorption redshift system at 0.4293 (E. Burbidge *et al.* 1977). Object 8 is three galaxies, for which Stockton (1974, 1978) has measured a redshift of 0.4340. The angular separation between the two QSOs is 4".8, which is 32 kpc at the absorption redshift. The galaxies are 10" or about 67 kpc from the low-redshift QSO.

We obtained *V*, *R*, and *I* exposures of this field with the video camera at the Cassegrain focus of the Mayall 4 m telescope. Examination of the three pictures indicates that the size of the image of the low-redshift QSO is larger relative to the high-redshift QSO in the *V* passband than in *R* or *I*; however, it is not apparent whether this effect is due to a difference in the colors of the two QSOs or the existence of extended emission around the low-redshift QSO. Since [O II]  $\lambda$ 3727 falls in the *V* passband and often appears strongly in nebulosity around QSOs, we undertook a seeing disk subtraction in an attempt to distinguish between the two explanations. The profile of the high-redshift QSO was scaled to have the same central intensity as the low-redshift QSO, and the two profiles were subtracted from the pictures in each passband. The *V* and *I* pictures after subtraction are shown in Figure 8 (Plate 13). The white dots are 1".15 in radius and represent the apparent seeing disk. The excess emission in the *V* exposure apparently arises in an extended region around the QSO, and appears to extend as far as the other QSO.

### III. DISCUSSION

Of the five QSOs and one BL Lacertae object listed in Table 2, the only existing evidence for "intervening material" is the absorption system in 1548+114*b* at a redshift which is approximately the same as the emission redshift of 1548+114*a* as well as the nearby group of objects studied by Stockton. However, it is just this object for which our "definitive test" becomes ambiguous, because it can be argued that the material projected onto 1548+114*b* was in fact ejected by 1548+114*a*; the excess emission described above suggests this. The fact that no Mg II absorption is seen in 1548+114*a* itself (E. Burbidge *et al.* 1977) could be ascribed to high ionization along the line of sight to 1548+114*a*. Empirically, it is known that Mg II absorption at the same redshift as the emission redshift in QSOs is exceedingly rare (Peterson and Strittmatter 1978).

Since we have not yet succeeded in obtaining redshifts for the objects near PHL 938 and 0952+179, and have not attempted to obtain spectra for any of the other nearby objects, we evidently cannot yet reach any conclusions on the origin of these low-*z* absorption systems.

Nevertheless, it is worth discussing the constraints which our data place on the origin of such systems as well as the likelihood of success of a spectroscopic investigation of the objects near the QSOs, since they are faint and will require considerable observing time. If the clouds responsible for the absorption are simply interstellar clouds within the disks of spiral or irregular galaxies, then one could attempt to detect either the

galaxy itself or nearby galaxies associated with the intervening galaxy. The data in Table 1 suggest that a typical galaxy at even our lowest redshift would be between 20.0 and 21.0  $m_p$ . Such an object would be very difficult to detect if it were superposed almost directly in front of the QSO. However, if the center of the galaxy were displaced by as little as 30 kpc, it would surely have been detected provided its absolute magnitude were brighter than about  $-19$ . However, if all the low-redshift ( $0.2 < z < 0.65$ ) systems detected in our spectroscopic survey to date are due simply to extended disks or halos of ordinary spirals, then the effective cross sections imply radii of at least  $\sim 100$  kpc (Weymann, Williams, and Peterson 1979). Thus we expect that the center of the galaxy whose hypothetical halo is responsible for the absorption should typically be at distances of this order from the line of sight to the QSO. The distance to the nearest object from each of the QSOs is shown in Table 2, and the mean value of this distance is  $\sim 85$  kpc. Alternatively, it is entirely possible that the clouds responsible for the absorption are not bound to individual galaxies at all but are intracluster clouds. The discovery of iron in roughly normal abundance in rich clusters is evidence that metal-enriched gas exists outside galaxies and can be readily explained by the ejection of material from galaxies during a early high-luminosity phase (De Young 1978). In the environment of rich clusters, this material soon thermalizes and remains very hot, but conceivably such material may condense into cool clouds if ejected from isolated galaxies in small groups. At ejection speeds of several hundred  $\text{km s}^{-1}$  the material would still be within a few Mpc of the parent group. How feasible would it be to detect the parent galaxies of such hypothetical clouds?

To investigate this question quantitatively, we consider the hypothesis that the cloud-galaxy spatial correlation function is identical to the two-point galaxy-galaxy spatial correlation. In particular, we assume the probability per unit (proper) volume of a galaxy whose luminosity is between  $L$ ,  $L \pm dL$  being found at a distance  $r$  from the hypothetical cloud to be

$$P(r; L; z)dLdV = \phi(x)(1+z)^{+3} \\ \times [1 + (1+z)^{-3}\xi(r)]dVdx. \quad (1)$$

In this expression  $x = L/L^*$ ,  $\phi(x)$  is Schechter's luminosity function (Schechter 1976), except that we have reduced the normalizing density  $\phi_0$  to a value of  $0.002/(\text{Mpc})^3$  following a rediscussion by Felten (1977). For the two-point correlation function  $\xi(r)$ , we adopt

$$\xi(r) = (r/7)^{-1.8} \quad r < 40 \text{ Mpc}, \\ = 0 \quad r > 40 \text{ Mpc}, \quad (2)$$

which is close to that found by Davis, Geller, and Huchra (1978). (Throughout this discussion  $H_0 = 50 \text{ km s}^{-1} \text{ Mpc}^{-1}$  and a  $q_0 = \frac{1}{2}$  universe has been assumed.) We adopt an absolute magnitude in the

TABLE 3  
PREDICTIONS OF CORRELATION MODEL

LIMITING MAGNITUDE ( $m_R$ )	RADIUS (arcsec)	"MEAN FIELD" GALAXIES	CORRELATED GALAXIES FOR CLOUDS AT VARIOUS $z$					
			0.1	0.2	0.3	0.4	0.5	0.6
20.0.....	15	0.059	0.098	0.051	0.022	0.007	0.001	0.000
	30	0.235	0.172	0.148	0.054	0.019	0.004	0.000
	45*	0.530	0.355	0.208	0.104	0.033	0.005	0.000
23.0.....	15	0.613	0.322	0.272	0.222	0.170	0.148	0.103
	30	2.453	0.564	0.789	0.538	0.481	0.355	0.216
	45*	5.520	1.168	1.107	1.041	0.810	0.558	0.325

\* For the purpose of comparison with this model and the results of Stockton (1978), a circle of radius 45" has been drawn around each of the QSOs in Figures 1 and 3-7.

red of  $-22.2$  for the  $L^*$  galaxies. The factor  $(1+z)^3$  outside the brackets accounts for the usual cosmological density increase, while the  $(1+z)^{-3}$  inside the brackets assumes that the gravitational interaction responsible for the correlation has offset the relative expansion of the clouds and galaxies since the epochs corresponding to  $z \lesssim 0.6$ .

In equation (1) the first term in the square brackets represents the contribution from the uncorrelated ("field") galaxies, and the second term represents the contribution from the correlated galaxies. With the assumptions described above we may integrate equation (1) over the appropriate galaxy luminosities and spatial volumes to find the number of field galaxies brighter than apparent magnitude  $m$ , as well as the number of galaxies correlated with an object at redshift  $z$  brighter than apparent magnitude  $m$ , both as a function of the field size surrounding the object. The results are, of course, also applicable to a search for companion galaxies if the intervening clouds are bound to an ordinary galaxy. Selected results are presented in Table 3. From inspection of this table it is seen that, if the correlation assumption described above is correct, then testing the hypothesis is likely to be a time-consuming task: even at redshifts as low as 0.2 the "correlated galaxies" are significantly outnumbered by the "field" galaxies, except for separations so small that the likelihood of finding any galaxies is small. This statement remains true for very faint limiting magnitudes.

Because of the atmospheric cutoff, it is not practical to carry out a search for Mg II absorption-line systems much below  $z = 0.2$ . Ca II H and K, can of course, be observed at very low redshifts, but we have found no such systems in our survey to date.

In view of the considerable uncertainties in our limiting magnitude and the results of Table 3 it is not possible to draw any conclusions concerning the likelihood that the "nearest neighbors" described above are actually "correlated galaxies." Nevertheless, we feel some further spectrographic effort on these objects is probably warranted, since it is entirely possible that the cloud-galaxy correlation may be stronger than assumed above.

In this connection it is of interest to apply the same considerations leading to Table 3 to recent work by

Stockton (1978). Stockton examined the field around 27 luminous QSOs with emission-line redshifts  $\leq 0.45$ . He found a total of 29 galaxies within a radius of 45" in these fields down to the limit of the red Palomar Sky Survey plates, which we assume to be  $m_R = 20.0$ . Of these 29 galaxies, Stockton obtained redshifts for 26 and assigned 13 of these to association with the QSOs on the basis of a velocity difference of less than  $1000 \text{ km s}^{-1}$ , i.e., half the galaxies studied were correlated. Assigning this same probability to all 29 galaxies we infer 14.5 "field" galaxies, or 0.54 per field, in very good agreement with the model represented in Table 3. However, if we compute the expected number of "correlated" galaxies by using the set of redshifts represented by Stockton's sample, we predict only about 2.4 correlated galaxies, far fewer than the number actually found by Stockton. *This suggests that galaxies may be more strongly correlated with QSOs than galaxies are correlated with other galaxies.* This result is in contrast to the result of Roberts, O'Dell, and Burbidge (1977), who examine the correlation between QSOs and rich clusters of galaxies.

#### IV. CONCLUSIONS

We present photographs of fields containing objects that are candidates for galaxies possibly associated with material producing low-redshift absorption lines in QSOs. At least two of the objects warrant further spectroscopic study. If the number of low-redshift Mg II absorption systems found in our QSO survey are all to be explained on the intervening hypothesis, then the typical separation of the optical image of the galaxy from the intervening cloud must be many tens of kpc—i.e., well separated from the QSO image. If the intervening clouds are not bound to individual galaxies and are correlated with galaxies with the same amplitude that galaxies are correlated with each other, then at these redshifts the "field galaxies" will significantly outnumber the "correlated galaxies." We stress this point because it implies that a substantial effort must be made before null results on redshift agreements can be used to rule out the correlation model described above. Finally, we conclude that the number of "correlated galaxies" found by Stockton

in fields surrounding low emission-line redshift QSOs is substantially higher than our correlation model predicts, implying either that the model is wrong or that galaxies are more strongly correlated with QSOs than with other galaxies.

We wish to thank Dr. C. R. Lynds for use of the plate reproduced in Figure 2 and Dr. H. Spinrad for obtaining the spectrum of object 5. We are indebted

to Drs. E. R. Craine and R. H. Cromwell for their help in the early stages of this work. One of us (T. A. B.) thanks Dr. W. L. W. Sargent for providing 4000 s of observing time on the Hale 5 m telescope and Dr. P. Goldreich for several helpful discussions. We thank Dr. P. L. Schechter for numerous stimulating discussions. This work has been supported by the National Science Foundation under grant AST 77-23055.

## REFERENCES

- Boksenberg, A., and Sargent, W. L. W. 1978, *Ap. J.*, **220**, 42.  
 Burbidge, E. M., and Burbidge, G. R. 1975, *Ap. J.*, **202**, 287.  
 Burbidge, E. M., Lynds, C. R., and Stockton, A. N. 1968, *Ap. J.*, **152**, 1077.  
 Burbidge, E. M., Smith, H. E., Weymann, R. J., and Williams, R. E. 1977, *Ap. J.*, **218**, 1.  
 Burbidge, E. M., and Strittmatter, P. A. 1972, *Ap. J. (Letters)*, **174**, L57.  
 Burbidge, G., O'Dell, S. L., Roberts, D. H., and Smith, H. E. 1977, *Ap. J.*, **218**, 33.  
 Carswell, R. F., Strittmatter, P. A., Williams, R. E., Kinman, T. D., and Serkowski, K. 1974, *Ap. J. (Letters)*, **190**, L101.  
 Coleman, G. D., and Weedman, D. W. 1978, private communication.  
 Davis, M., Geller, M. J., and Huchra, J. 1978, *Ap. J.*, **221**, 1.  
 De Young, D. S. 1978, preprint.  
 Felten, J. E. 1977, *A.J.*, **82**, 861.  
 Grewing, M., and Mebold, U. 1975, *Astr. Ap.*, **42**, 119.  
 Haschick, A. D., and Burke, B. F. 1975, *Ap. J. (Letters)*, **200**, L137.  
 Hazard, C., Gulkis, S., and Bray, A. D. 1967, *Ap. J.*, **148**, 669.  
 Holmberg, E. 1975, in *Galaxies and the Universe*, ed. A. Sandage, M. Sandage, and J. Kristian (Chicago: University of Chicago Press), p. 123.  
 Kinman, T. D., and Burbidge, E. M. 1967, *Ap. J. (Letters)*, **148**, L59.  
 Lynds, C. R. 1967, *Ap. J.*, **147**, 396.  
 Pence, W. 1976, *Ap. J.*, **203**, 39.  
 Penston, M. V. 1976, private communication.  
 Peterson, B. M. 1978, *Ap. J.*, **223**, 740.  
 Peterson, B. M., Coleman, G. D., Strittmatter, P. A., and Williams, R. E. 1977, *Ap. J.*, **218**, 605.  
 Peterson, B. M., and Strittmatter, P. A. 1978, *Ap. J.*, **226**, in press.  
 Roberts, D. H., O'Dell, S. L., and Burbidge, G. R. 1977, *Ap. J.*, **216**, 227.  
 Schechter, P. 1976, *Ap. J.*, **203**, 297.  
 Stockton, A. 1974, *Nature*, **250**, 308.  
 ———. 1978, *Ap. J.*, **223**, 747.  
 Tinsley, B. 1976, *Ap. J. (Letters)*, **210**, L49.  
 Turnrose, B. E. 1974, *Pub. A.S.P.*, **86**, 545.  
 Wampler, E. J., Baldwin, J. A., Burke, W. L., Robinson, L. B., and Hazard, C. 1973, *Nature*, **246**, 203.  
 Wells, D. 1975, *KPNO and CTIO Quarterly Bull.*, July-September, p. 12.  
 Weymann, R. J., Williams, R. E., and Peterson, B. M. 1979, in preparation.

TODD A. BOROSON, BRADLEY M. PETERSON, and RAY J. WEYMANN: Steward Observatory, University of Arizona, Tucson, AZ 85721

HARVEY R. BUTCHER: Kitt Peak National Observatory, P.O. Box 26732, Tucson, AZ 85726

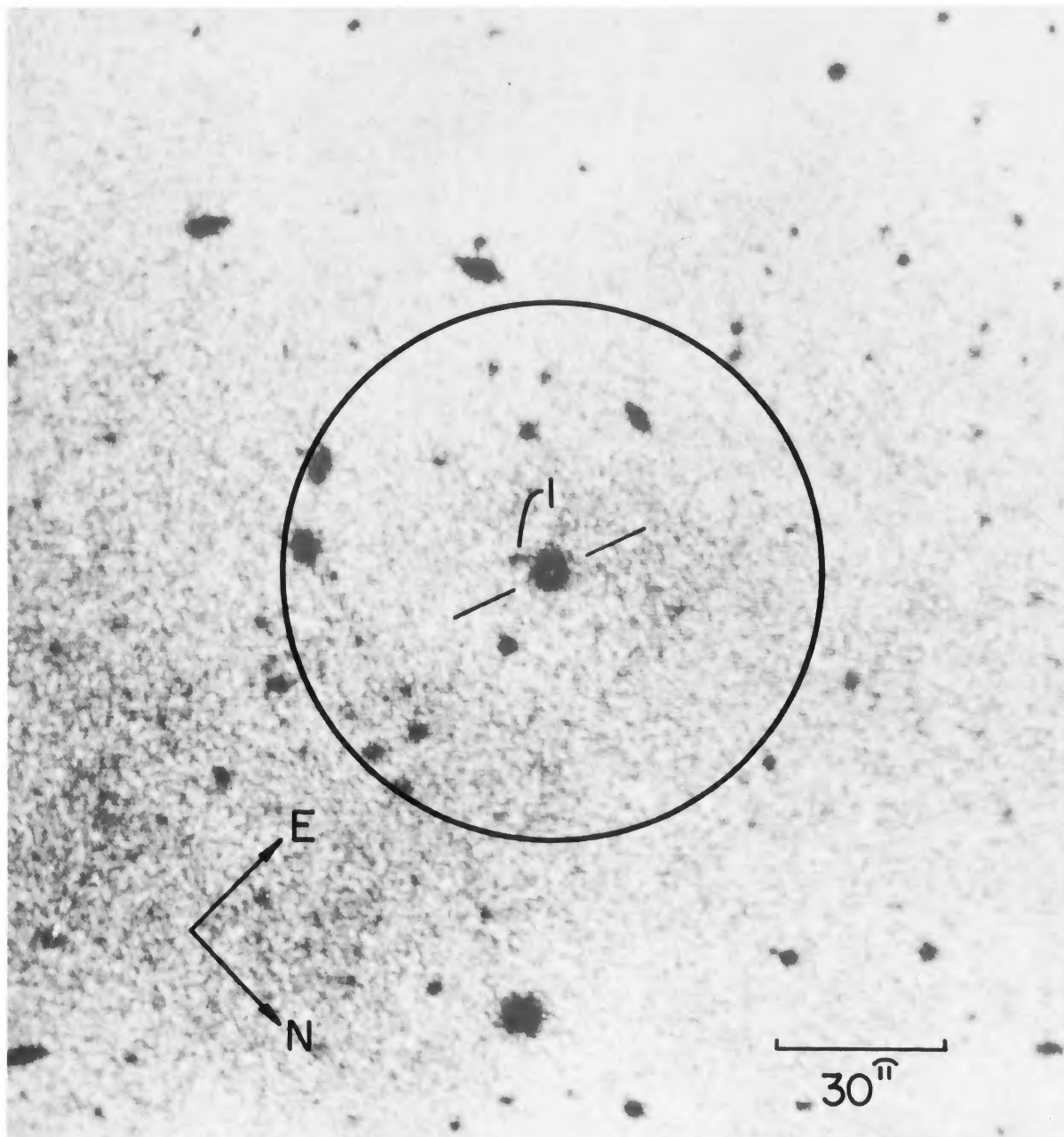


FIG. 1.—Composite picture of the field of the QSO PHL 938. The QSO is the object indicated at the center of the field. The numbered object is discussed in the text. A  $45''$  radius circle centered on the QSO has been drawn to facilitate comparison with the predictions of the model discussed in § III of the text.

WEYMANN *et al.* (see page 604)

## PLATE 7

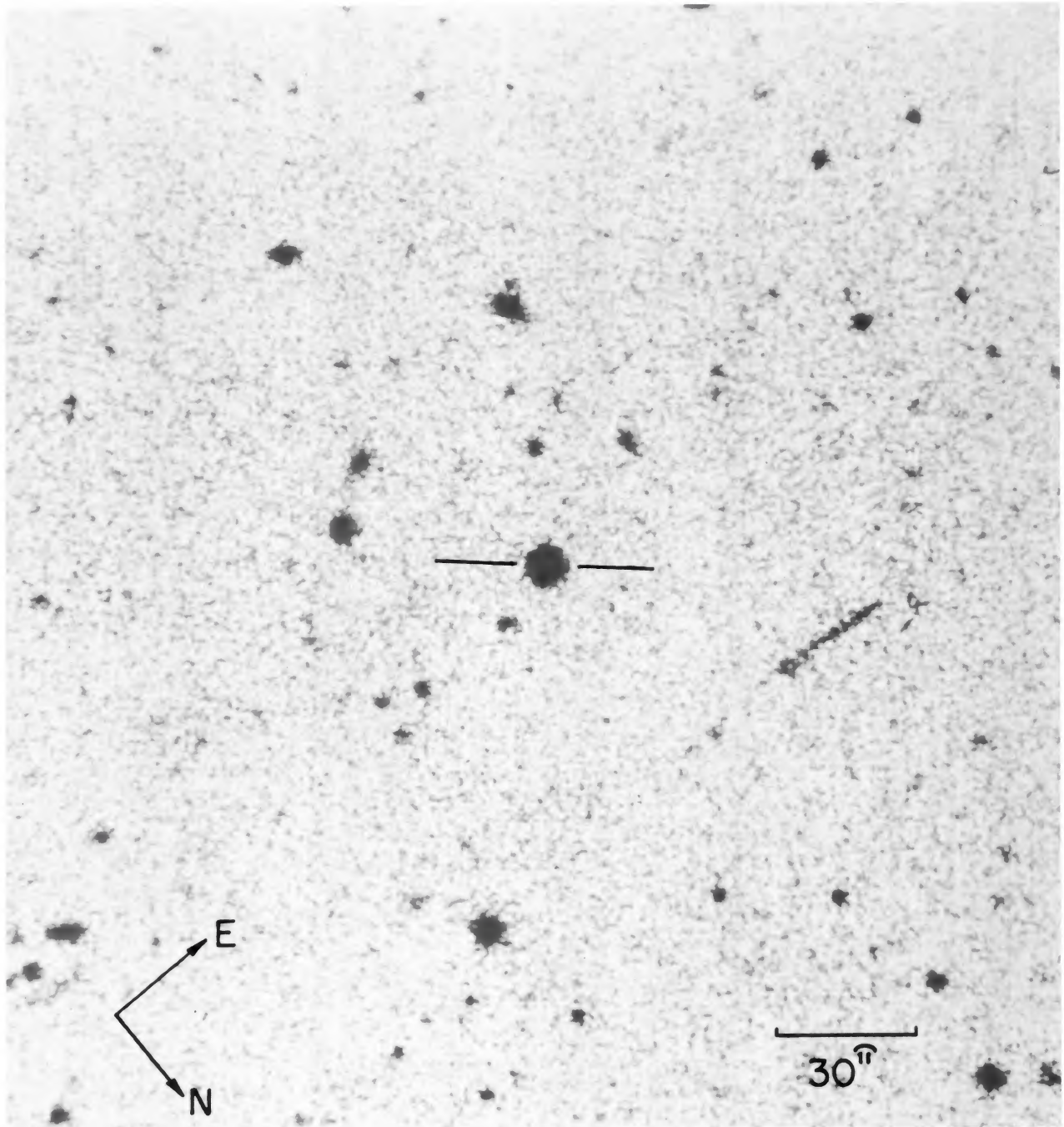


FIG. 2.—Blue photograph (IIIa-J + GG385) of the field of the QSO PHL 938, taken by C. R. Lynds with the Mayall 4 m telescope.

WEYMANN *et al.* (see page 605)

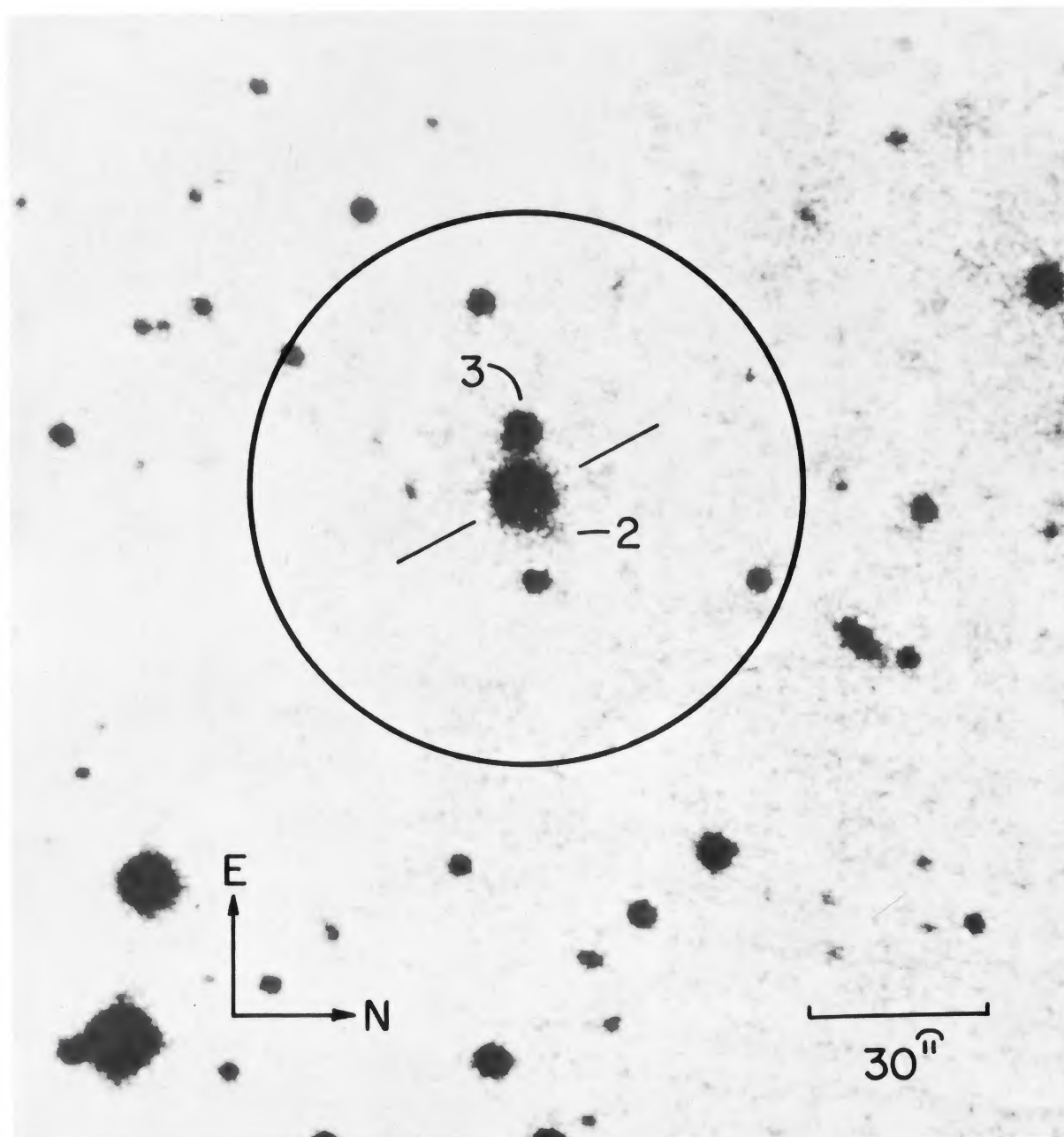


FIG. 3.—Red photograph of the field of the BL Lacertae object PKS 0735+178. Features are indicated as in Fig. 1. WEYMANN *et al.* (see page 605)

## PLATE 9

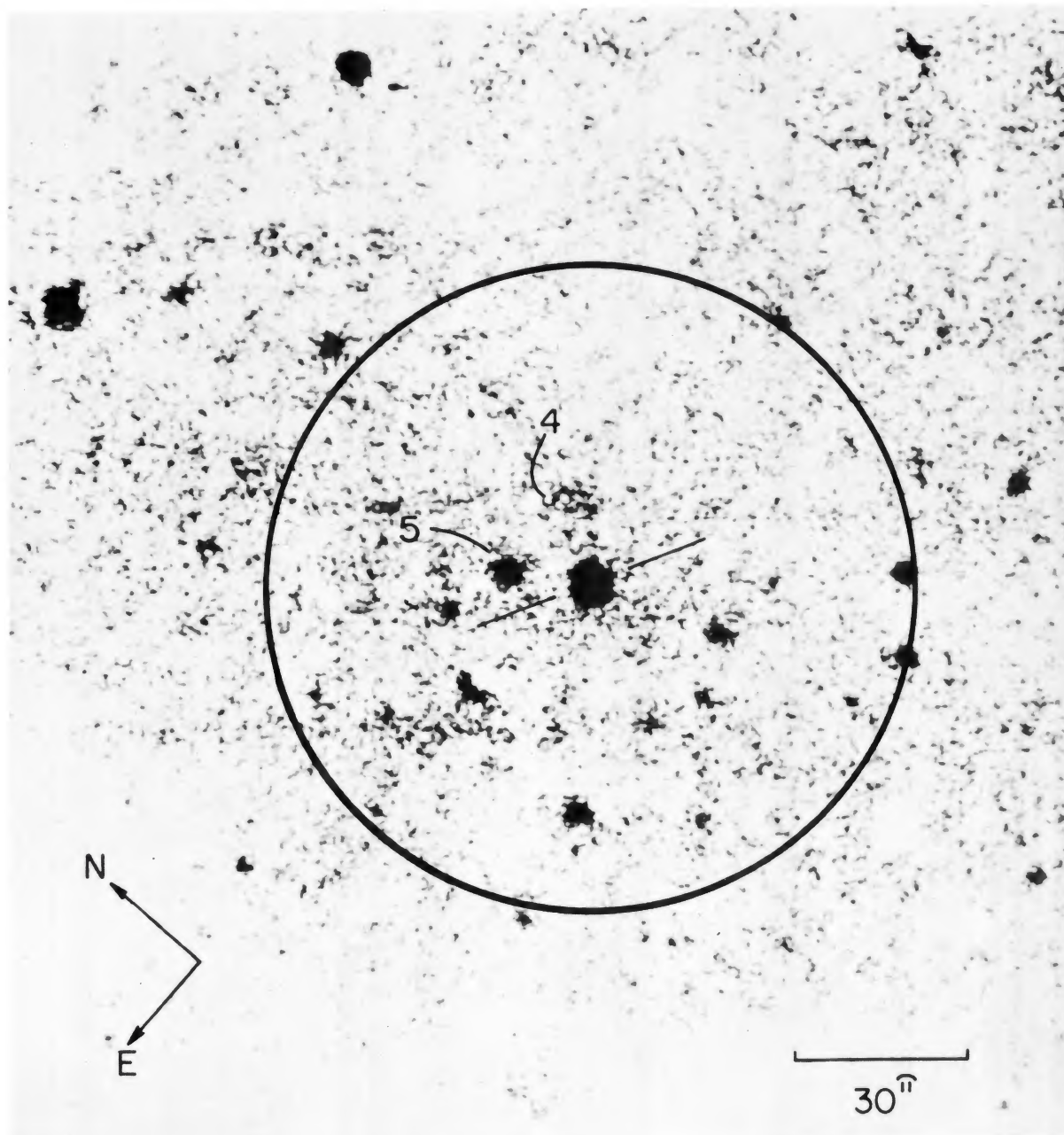


FIG. 4.—Composite picture of the field of the QSO AO 0952+179. Features are indicated as in Fig. 1.  
WEYMANN *et al.* (see page 605)

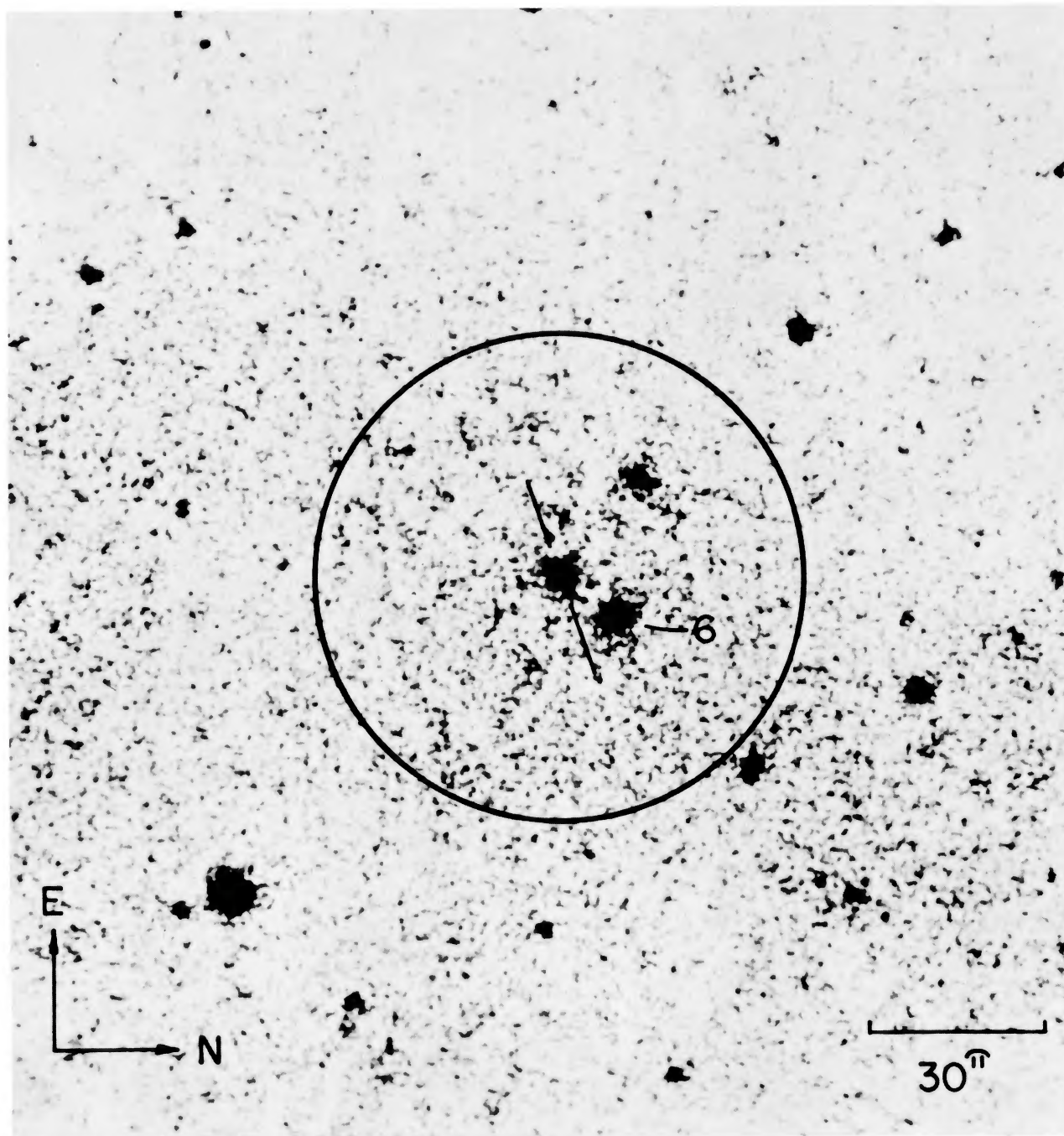


FIG. 5.—Composite picture of the field of the QSO 4C 06.41. Features are indicated as in Fig. 1.  
WEYMANN *et al.* (see page 605)

## PLATE 11

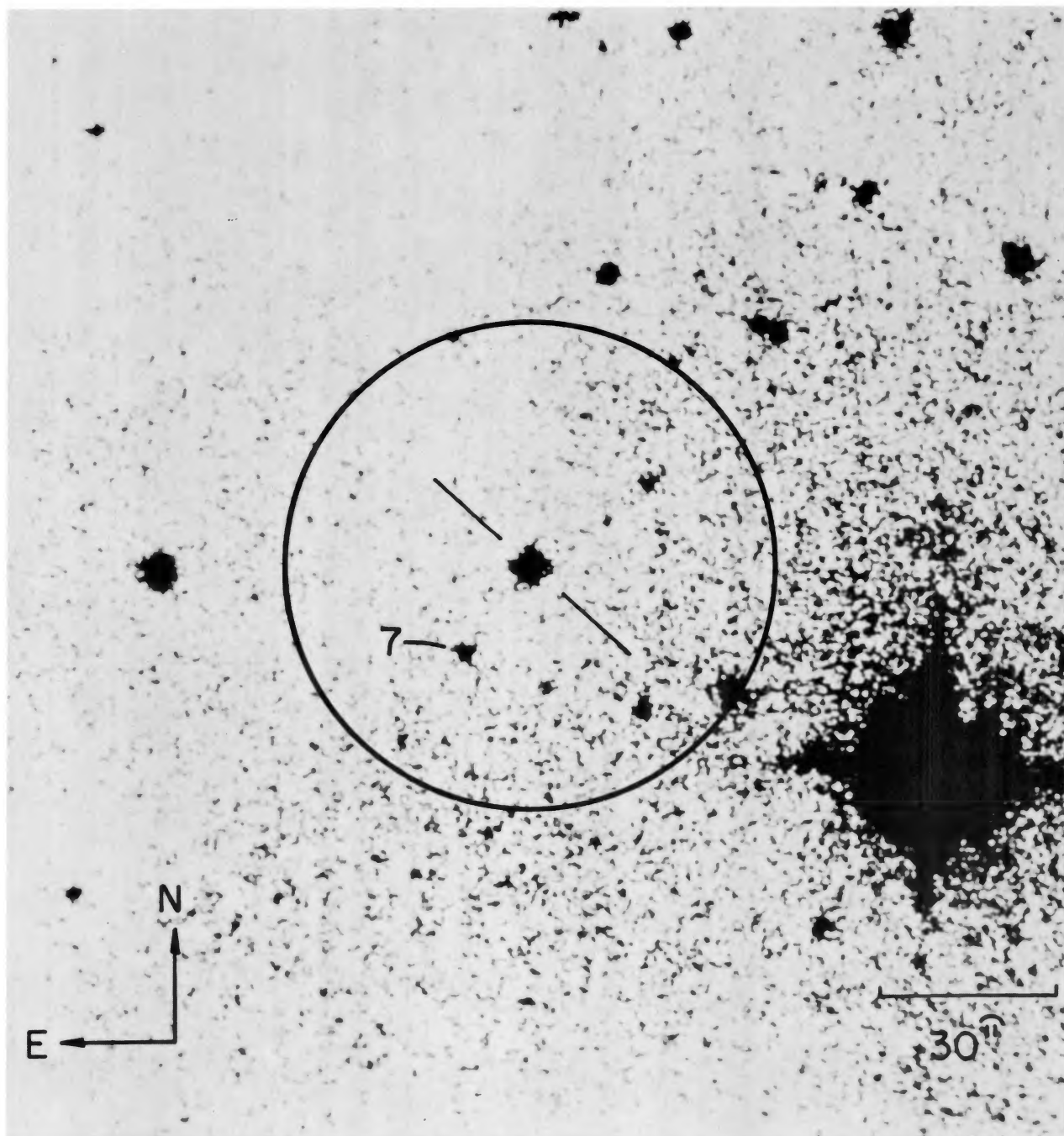


FIG. 6.—Composite picture of the field of the QSO PKS 1229–02. Features are indicated as in Fig. 1.  
WEYMANN *et al.* (see page 605)

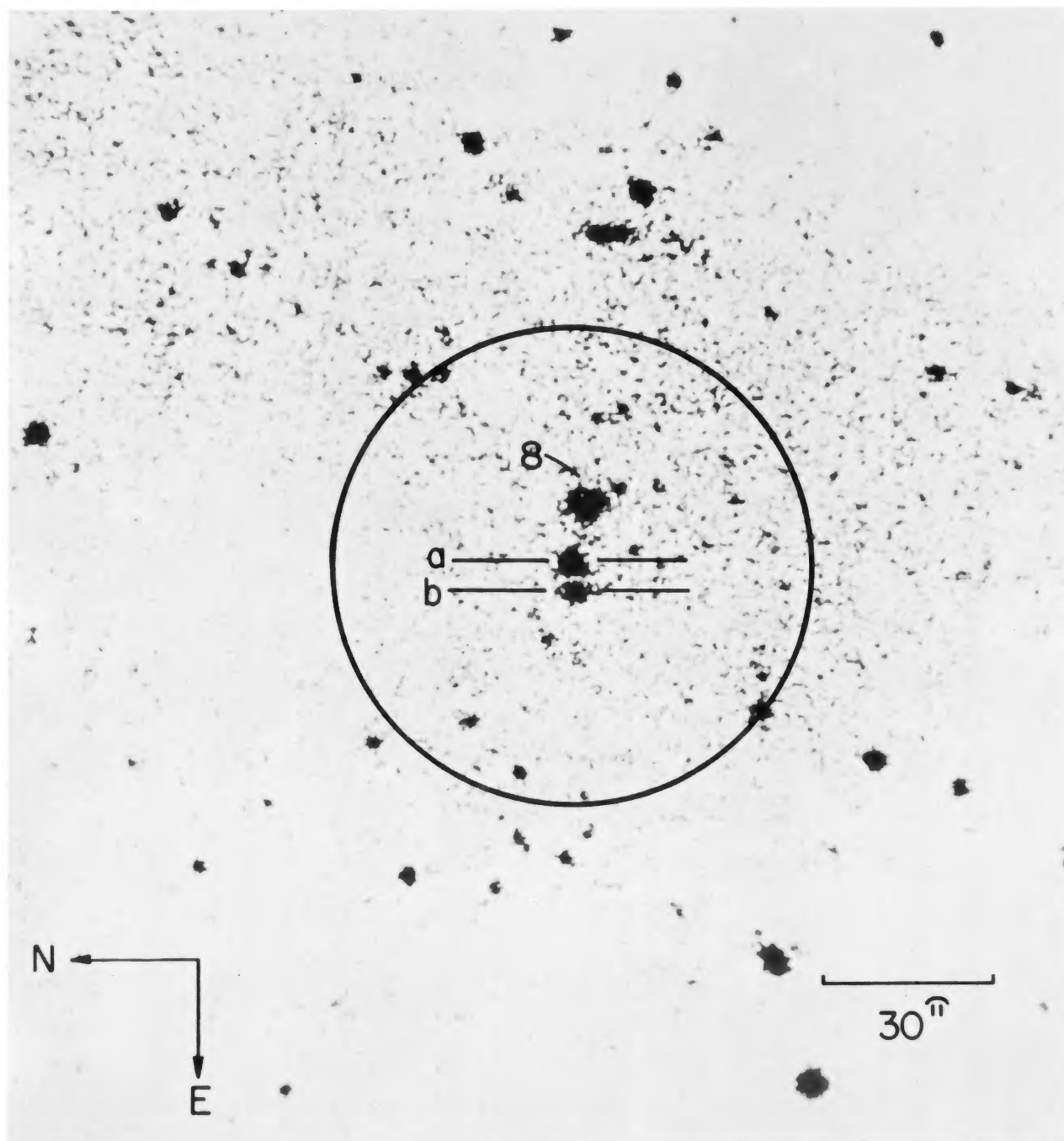


FIG. 7.—Composite picture of the field of the double QSO 1548+114. Features are indicated as in Fig. 1.  
WEYMANN *et al.* (see page 605)

## PLATE 13

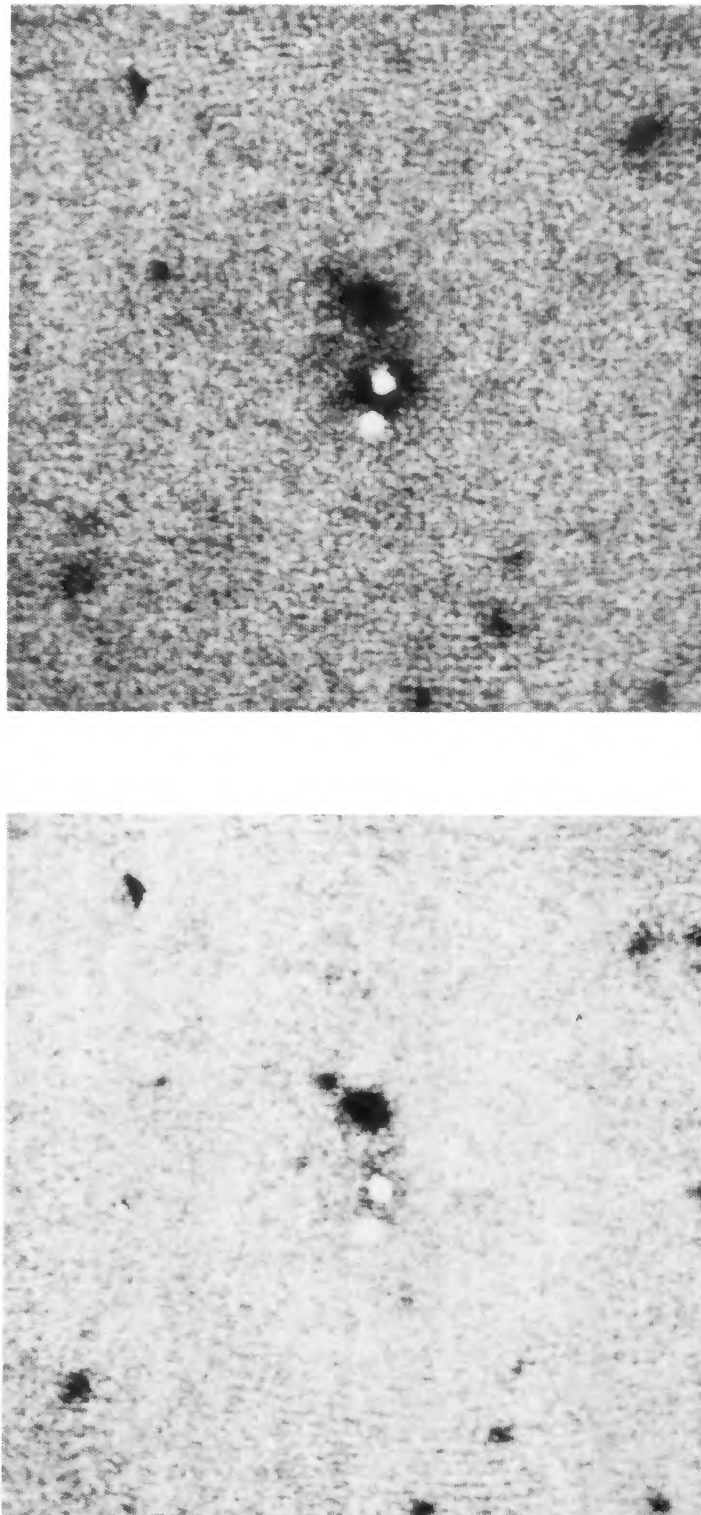


FIG. 8.—Video camera picture of the field of the double QSO 1548 + 114 in  $V$  (upper) and  $I$  (lower) after seeing disk subtraction (see text).

WEYMANN *et al.* (see page 606)